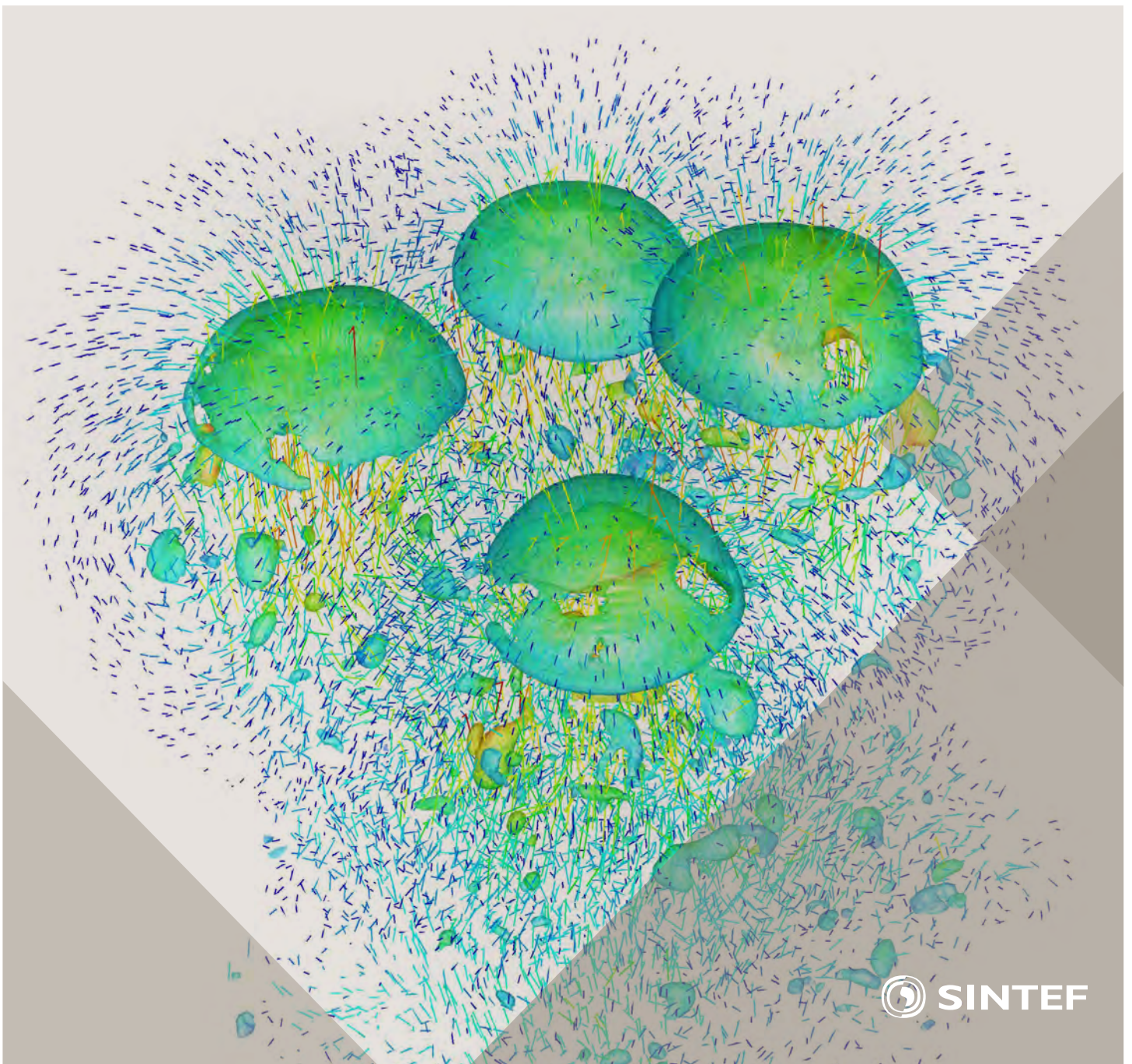


Selected papers from 10<sup>th</sup> International Conference on  
Computational Fluid Dynamics in the Oil & Gas, Metal-  
lurgical and Process Industries

# Progress in Applied CFD



SINTEF Proceedings

Editors:

Jan Erik Olsen and Stein Tore Johansen

## **Progress in Applied CFD**

Selected papers from 10<sup>th</sup> International Conference on Computational Fluid  
Dynamics in the Oil & Gas, Metallurgical and Process Industries

SINTEF Academic Press

SINTEF Proceedings no 1

Editors: Jan Erik Olsen and Stein Tore Johansen

**Progress in Applied CFD**

Selected papers from 10<sup>th</sup> International Conference on Computational Fluid Dynamics in the Oil & Gas, Metallurgical and Process Industries

Key words:

CFD, Flow, Modelling

Cover, illustration: Rising bubbles by Schalk Cloete

ISSN 2387-4287 (printed)

ISSN 2387-4295 (online)

ISBN 978-82-536-1432-8 (printed)

ISBN 978-82-536-1433-5 (pdf)

60 copies printed by AIT AS e-dit

Content: 100 g munken polar

Cover: 240 g trucard

© Copyright SINTEF Academic Press 2015

The material in this publication is covered by the provisions of the Norwegian Copyright Act. Without any special agreement with SINTEF Academic Press, any copying and making available of the material is only allowed to the extent that this is permitted by law or allowed through an agreement with Kopinor, the Reproduction Rights Organisation for Norway. Any use contrary to legislation or an agreement may lead to a liability for damages and confiscation, and may be punished by fines or imprisonment

SINTEF Academic Press

Address:       Forskningsveien 3 B  
                  PO Box 124 Blindern  
                  N-0314 OSLO

Tel:             +47 22 96 55 55

Fax:            +47 22 96 55 08

[www.sintef.no/byggforsk](http://www.sintef.no/byggforsk)

[www.sintefbok.no](http://www.sintefbok.no)

**SINTEF Proceedings**

SINTEF Proceedings is a serial publication for peer-reviewed conference proceedings on a variety of scientific topics.

The processes of peer-reviewing of papers published in SINTEF Proceedings are administered by the conference organizers and proceedings editors. Detailed procedures will vary according to custom and practice in each scientific community.

## PREFACE

This book contains selected papers from the 10<sup>th</sup> International Conference on Computational Fluid Dynamics in the Oil & Gas, Metallurgical and Process Industries. The conference was hosted by SINTEF in Trondheim in June 2014 and is also known as CFD2014 for short. The conference series was initiated by CSIRO and Phil Schwarz in 1997. So far the conference has been alternating between CSIRO in Melbourne and SINTEF in Trondheim. The conferences focus on the application of CFD in the oil and gas industries, metal production, mineral processing, power generation, chemicals and other process industries. The papers in the conference proceedings and this book demonstrate the current progress in applied CFD.

The conference papers undergo a review process involving two experts. Only papers accepted by the reviewers are presented in the conference proceedings. More than 100 papers were presented at the conference. Of these papers, 27 were chosen for this book and reviewed once more before being approved. These are well received papers fitting the scope of the book which has a slightly more focused scope than the conference. As many other good papers were presented at the conference, the interested reader is also encouraged to study the proceedings of the conference.

The organizing committee would like to thank everyone who has helped with paper review, those who promoted the conference and all authors who have submitted scientific contributions. We are also grateful for the support from the conference sponsors: FACE (the multiphase flow assurance centre), Total, ANSYS, CD-Adapco, Ascomp, Statoil and Elkem.

Stein Tore Johansen & Jan Erik Olsen



Organizing committee:

Conference chairman: Prof. Stein Tore Johansen

Conference coordinator: Dr. Jan Erik Olsen

Dr. Kristian Etienne Einarsrud

Dr. Shahriar Amini

Dr. Ernst Meese

Dr. Paal Skjetne

Dr. Martin Larsson

Dr. Peter Witt, CSIRO

Scientific committee:

J.A.M. Kuipers, TU Eindhoven

Olivier Simonin, IMFT/INP Toulouse

Akio Tomiyama, Kobe University

Sanjoy Banerjee, City College of New York

Phil Schwarz, CSIRO

Harald Laux, Osram

Josip Zoric, SINTEF

Jos Derksen, University of Aberdeen

Dieter Bothe, TU Darmstadt

Dmitry Eskin, Schlumberger

Djamel Lakehal, ASCOMP

Pär Jonsson, KTH

Ruben Shulkes, Statoil

Chris Thompson, Cranfield University

Jinghai Li, Chinese Academy of Science

Stefan Pirker, Johannes Kepler Univ.

Bernhard Müller, NTNU

Stein Tore Johansen, SINTEF

Markus Braun, ANSYS

# CONTENTS

<b>Chapter 1: Pragmatic Industrial Modelling</b> .....	<b>7</b>
On pragmatism in industrial modeling .....	9
Pragmatic CFD modelling approaches to complex multiphase processes.....	25
A six chemical species CFD model of alumina reduction in a Hall-Hérault cell .....	39
Multi-scale process models to enable the embedding of CFD derived functions: Curtain drag in flighted rotary dryers .....	47
<b>Chapter 2: Bubbles and Droplets</b> .....	<b>57</b>
An enhanced front tracking method featuring volume conservative remeshing and mass transfer .....	59
Drop breakup modelling in turbulent flows .....	73
A Baseline model for monodisperse bubbly flows .....	83
<b>Chapter 3: Fluidized Beds</b> .....	<b>93</b>
Comparing Euler-Euler and Euler-Lagrange based modelling approaches for gas-particle flows.....	95
State of the art in mapping schemes for dilute and dense Euler-Lagrange simulations .....	103
The parametric sensitivity of fluidized bed reactor simulations carried out in different flow regimes.....	113
Hydrodynamic investigation into a novel IC-CLC reactor concept for power production with integrated CO <sub>2</sub> capture .....	123
<b>Chapter 4: Packed Beds</b> .....	<b>131</b>
A multi-scale model for oxygen carrier selection and reactor design applied to packed bed chemical looping combustion .....	133
CFD simulations of flow in random packed beds of spheres and cylinders: analysis of the velocity field .....	143
Numerical model for flow in rocks composed of materials of different permeability.....	149
<b>Chapter 5: Metallurgical Applications</b> .....	<b>157</b>
Modelling argon injection in continuous casting of steel by the DPM+VOF technique.....	159
Modelling thermal effects in the molten iron bath of the HIs melt reduction vessel.....	169
Modelling of the Ferrosilicon furnace: effect of boundary conditions and burst .....	179
Multi-scale modeling of hydrocarbon injection into the blast furnace raceway.....	189
Prediction of mass transfer between liquid steel and slag at continuous casting mold .....	197
<b>Chapter 6: Oil &amp; Gas Applications</b> .....	<b>205</b>
CFD modeling of oil-water separation efficiency in three-phase separators.....	207
Governing physics of shallow and deep subsea gas release .....	217
Cool down simulations of subsea equipment.....	223
Lattice Boltzmann simulations applied to understanding the stability of multiphase interfaces.....	231
<b>Chapter 7: Pipeflow</b> .....	<b>239</b>
CFD modelling of gas entrainment at a propagating slug front.....	241
CFD simulations of the two-phase flow of different mixtures in a closed system flow wheel.....	251
Modelling of particle transport and bed-formation in pipelines .....	259
Simulation of two-phase viscous oil flow .....	267



## PREDICTION OF MASS TRANSFER BETWEEN LIQUID STEEL AND SLAG AT CONTINUOUS CASTING MOULD

Pascal GARDIN<sup>1\*</sup>, Ségolène GAUTHIER<sup>1</sup>, Stéphane VINCENT<sup>2</sup>

<sup>1</sup> ArcelorMittal Global R&D, 57283 Maizières-lès-Metz, FRANCE

<sup>2</sup> I2M, Trèfle department, 33607 Pessac, FRANCE

\* E-mail: pascal.gardin@arcelormittal.com

### ABSTRACT

For the prediction of steel desulphurization and dephosphorization or the evolution of slag composition at continuous casting mould, mass transfer between two immiscible fluids in a turbulent situation should be calculated.

For this purpose, two possibilities are offered for the simulation. The first one consists in the calculation of the local chemical equilibrium with the simultaneous prediction of the species transport, but the cost is that very fine mesh should be used. The second is based on the assessment of the mass transfer coefficient from hydrodynamic calculations and further use of thermodynamic code fed with interface area and transfer coefficients. On a computing time point of view, this second method is more affordable for 3D configurations than the first one, but it is less accurate. Literature survey indicates that it is possible to obtain a realistic evaluation of the mass transfer coefficient from hydrodynamic calculations, under the condition of very precise description of the flow near the interface.

The paper explains the reasons for the different simplifications which were made to predict the mass transfer between liquid steel and slag, gives indication on interest and limitation of the coupling between fluid dynamics and thermodynamics to get the local and time dependent evolution of chemical composition in the two phases. The modelling to predict the mass transfer coefficient is also described and compared to correlation proposed in the literature. Finally, a correlation is proposed to get mass transfer coefficient up to Schmidt number = 1000.

**Keywords:** CFD, Pragmatic industrial modelling, Multiphase Heat and Mass transfer, Casting, Slag.

### NOMENCLATURE

#### Greek Symbols

$\Lambda$  Integral length scale of turbulence, [m].

$\delta_s$  Thickness of species boundary layer, [m].

$\delta_m$  Thickness of momentum boundary layer, [m].

$\mu$  Dynamic viscosity, [kg/m.s].

$\beta$  Mass transfer coefficient, [m/s].

$\Delta z$  Cell thickness near interface, [m].

#### Latin Symbols

C Non-dimensional concentration.

D Mass diffusivity, [m<sup>2</sup>/s].

H Half height of the channel, [m].

Sc Schmidt number.

u\* Friction velocity at interface, [m/s].

u<sub>max</sub> Maximum velocity in the phase, [m/s].

#### Sub/superscripts

G Gas phase.

i Interface.

ls Liquid steel.

sl Slag.

$\infty$  Far from interface.

### INTRODUCTION

All along the steel refining route and casting, the liquid steel is rarely exposed to the ambient atmosphere. It is often covered with a thermal insulation: the slag. This is the case in a continuous casting mould, which is the reactor largely used to solidify steel. Figure 1 gives a schematic diagram of the operation and the various phases present in a mould:

- the liquid steel, also carrying argon bubbles and micro-particles coming from an endogenous precipitation in the liquid steel, is introduced through a nozzle into the mould ( typical section of 1800 \* 220 mm<sup>2</sup> ), the value of the Reynolds number at the outlet nozzle is in the order of 70000, which produces a high degree of turbulence in the mould and at the interface between liquid metal-slag; the argon bubbles limit the clogging phenomena inside the nozzle and strongly disturb the liquid steel / slag interface when crossing.



- the flux powder is deposited continuously on the upper surface and at about 1000 °C, it liquefies over a thickness of a few millimetres to form the liquid slag.

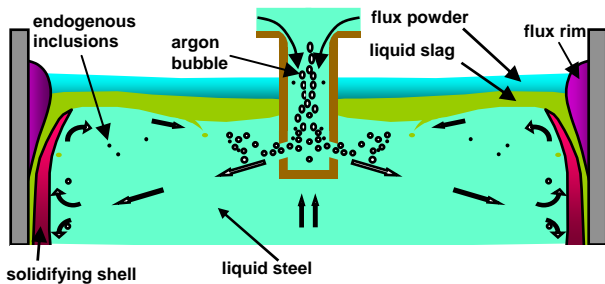


**Figure 1:** Different phases in a continuous casting mould, Pericleous (2008).

In a mould, the liquid slag has another specific function: it is entrained between the mould and the solidifying skin and facilitates lubrication. In the latter case, it is important to control the composition of the slag, to guarantee its good viscosity and its ability to lubricate. Another characteristic is that the slag should not be fragmented; if slag droplets are suspended in the liquid steel, they can be entrapped by the solidifying shell and produce surface defects on the final product. It is currently one of the major defects in our steel plants.

New steels grades (such as Advanced High-Strength Steel) contain alloying elements that can affect the slag behaviour; for example, depending on the aluminium mass fraction inside the liquid steel,  $\text{Al}_2\text{O}_3$  content of the slag can vary between 3-4 % and 30-35 %, which deeply affects its viscosity (multiplied by 5), Shahbazian et al. (2002), and its thermal conductivity, modifying the extraction of the heat flux through the mould. Robustness issues of the process are then encountered; if the viscosity increases, the quality of the lubrication is degraded, which leads to a rupture of the slag film and a direct contact of the molten steel with the mould: if a sticking takes place, it may be impossible to extract continuously the steel from the mould and the process should be stopped and the mould replaced.

Process control means that mass transfer should be controlled to have insight into the chemical evolution of the slag. In this context, we have to control the dynamic behaviour of the interface between liquid steel and slag and detect if interface fragmentation will occur or not, since it will affect interfacial area for mass transfer and steel quality if slag droplets are entrapped by the solidifying shell. Several mechanisms are involved in the fragmentation, which is already the subject of dedicated studies, Hagemann (2013), Real-Ramirez (2011). Figure 2 shows a typical interface behaviour observed in a water model. Part of the flow coming from the nozzle is deviated towards the interface and, above a critical water velocity, the interface is strongly distorted and can be fragmented. Another mechanism can be observed: the creation of a drainage cone which

can produce small droplets of the upper phase in the lower one when it breaks.

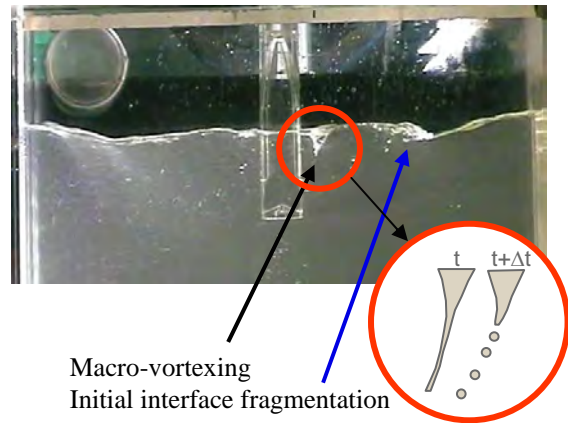


**Figure 2:** Typical behaviour of interface.

Mass transfer across a turbulent interface has already been investigated. In the steelmaking community, KTH teams have published some papers showing the evolution of slag compositions interacting with the liquid metal, Jonsson (1998), Andersson (2002), Doostmohammadi (2010).

However, as soon as CFD and thermodynamics are coupled, it is difficult to understand in details the numerical procedure for the coupling and there is a too brief discussion on different topics: dependence of the result to the mesh size and treatment of the interfacial turbulence (on the basis of RANS turbulence models). Although the method is qualitatively interesting, further investigations are necessary.

To get the mass transfer coefficient, different teams proposed interesting papers based on CFD calculations. In the case of a plane interface between water and liquid Calmet (1998) has shown the relevance of using a LES turbulence model to describe the interface with and without shear stress, and to identify the coefficient of mass transfer up to Schmidt number 200. More recently, Figueroa-Espinoza (2010) extended the method to predict the mass transfer between a bubble with a variable shape, using a mesh conforming to the shape of the bubble, for values of the Schmidt number up to 500.

Banerjee (2004) also took into account the deformation of the interface and made calculations for Schmidt numbers up to 10-20; he proposed the promising “surface divergence” model for deriving the mass transfer coefficient.

## EVOLUTION OF CHEMICAL COMPOSITION

The objective is to get the time evolution of the steel and slag compositions. We have to calculate the flow, the local composition and advection/diffusion of the different chemical species, but also the chemical reactions between steel and slag. Ansys-Fluent™ predicts the flow of liquid steel and slag phases with the Volume Of Fluid model, each phase being constituted of a mix of several species. An in-house code is used for the thermodynamics calculations. Because

precipitation and chemical compositions in liquid or solid steel are very specific, ArcelorMittal R&D developed its own code, called CEQCSI, for Chemical EQUilibrium Calculation for the Steel Industry. It allows the calculation of local compositions and precipitations of different oxides ( $\text{SiO}_2$  -  $\text{TiO}_2$  -  $\text{Ti}_2\text{O}_3$  -  $\text{Cr}_2\text{O}_3$  -  $\text{Al}_2\text{O}_3$  -  $\text{Fe}_2\text{O}_3$ - $\text{CrO}$  -  $\text{FeO}$  -  $\text{MgO}$  -  $\text{MnO}$  -  $\text{CaO}$ ...) and slag-metal reactions, Lehmann (2008).

By means of User Defined Functions that can be addressed in Ansys-Fluent™, we can detect the cells where slag and steel are both present; mass fraction of the different species at time t are sent to Ceqcsi which makes the calculations for the new equilibrium composition in each phase and then gives the resulting source terms for each species to Ansys-Fluent™. Advection/diffusion takes place during  $\Delta t$  and new composition is calculated in the entire domain at  $t+\Delta t$  by Ceqcsi. With this iterative procedure, it is possible to have the time evolution of the chemical composition in each phase.

We initiated calculations in 2D. The geometry of the top region is displayed on Figure 3. The height is 1500 mm and width is 800 mm. Initial slag thickness is 50 mm. The number of cells, for the initial calculations is 21600. VOF-PLIC method is used to predict the interface and realisable k- $\epsilon$  is selected for turbulence modelling. Turbulence damping at interface is considered by means of a source term in the  $\epsilon$  transport equation, Gardin (2011). Because slag is consumed to lubricate the mould, we impose slag inlet along the horizontal top line (Velocity inlet (1)) and slag is extracted by the two vertical segments (Velocity inlet (2)) with the composition of adjacent cells and negative velocity to get outlet conditions. Slag can be consumed or created due to the composition adjustment calculated by Ceqcsi; it means that slag volume, and by consequence steel volume, can change with time according to the chemical equilibrium with steel. The consequence is also that thermodynamics should be coupled with fluid flow calculations at each time step: unfortunately, freezing the steel/slag interface for further thermodynamics calculations is not possible and transient calculations should be performed.

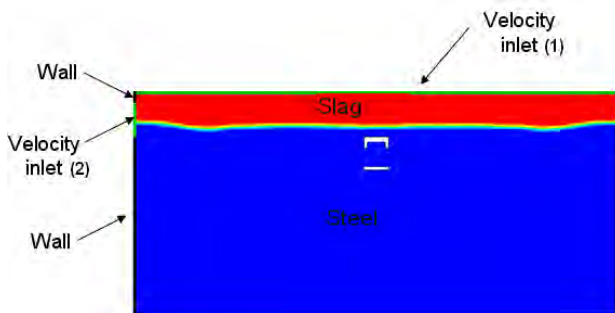


Figure 3: Top region of the calculation domain with boundary conditions.

Figure 4 illustrates the 2D velocity field that we obtained. The slag movement is mainly due to momentum transfer from liquid steel to slag at interface.

The impact of slag injection by the top on slag movement is very small.

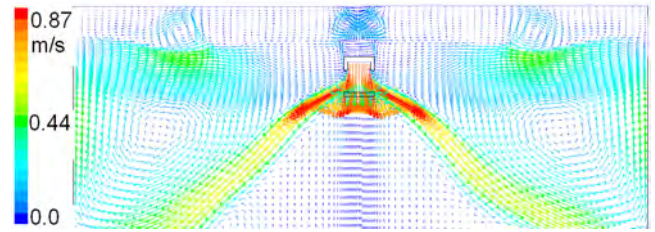


Figure 4: Typical velocity field in steel and slag.

The coupling between Ansys-Fluent™ and Ceqcsi was applied with the composition of steel and slag as it is expressed in Table 1 at  $t=0$  s.

Table 1: Initial steel and slag compositions.

species	Steel %wt	Slag %wt
Fe	98.8273	
Al	0.031	
Mn	/	
Si	/	
Ca	/	
S	/	
O	0.0005	
$\text{SiO}_2$		38
$\text{Al}_2\text{O}_3$		9
$\text{Fe}_2\text{O}_3$		/
FeO	/	/
MnO		/
MgO		/
CaO		27
$\text{CaF}_2$		/

As we can see on Figure 5, Al distribution in the mould is heterogeneous after 113 s of calculation, especially near the interface. Al is transported towards the interface and there is a progressive Al consumption to form  $\text{Al}_2\text{O}_3$  in the slag; in consequence, there is a progressive decrease of Al concentration as the flow transports Al along the interface towards the centre of the mould.

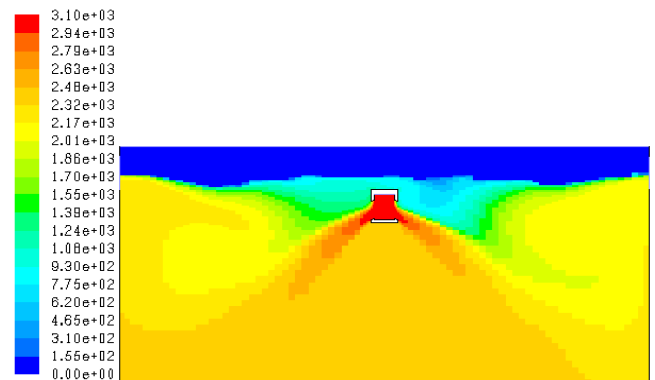
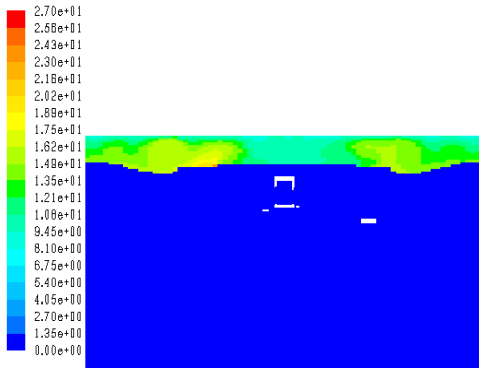


Figure 5: Mass fraction of Al (ppm) at  $t=113$  s – time step for CEQCSI call: 0.05 s.

The Al distribution in liquid steel should be related to the alumina distribution in the slag (Figure 6) which also displays important variations; it is observed low

Al<sub>2</sub>O<sub>3</sub> concentration in low velocity regions: mixing by advection/diffusion is too slow with the consequence of slag viscosity heterogeneously distributed.



**Figure 6:** Mass fraction of Al<sub>2</sub>O<sub>3</sub> (ppm) at t=113 s – time step for CEQCSI call: 0.05 s.

Analysis of the influence of the mesh size near the interface was realized. Initial mesh which was used for the previous results is displayed on Figure 7. Then, cells are successively divided by 2 and 4 in the region containing the interface. Cell thickness is respectively 4, 2 and 1 mm.

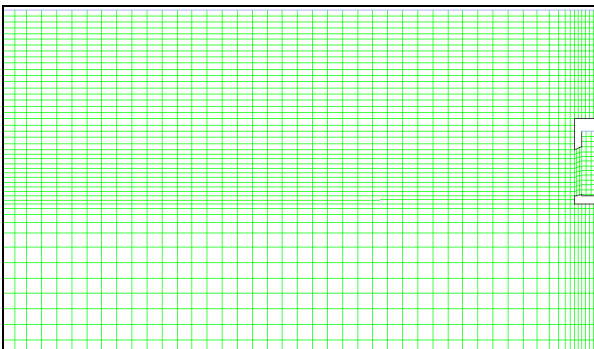


**Figure 7:** Initial mesh – half geometry is considered

The time step between two successive Ceqcsi calls is maintained constant to 0.05s and mean Al<sub>2</sub>O<sub>3</sub> content in the slag is drawn for the three cases. Figure 8 clearly shows that results are strongly mesh dependent and that stationary concentration is more rapidly obtained for large mesh. If time step to call Ceqcsi is decreased, other calculations show that Al<sub>2</sub>O<sub>3</sub> evolution is quicker than with 0.05s. At this stage, we conclude that results are mesh and time-step dependent.

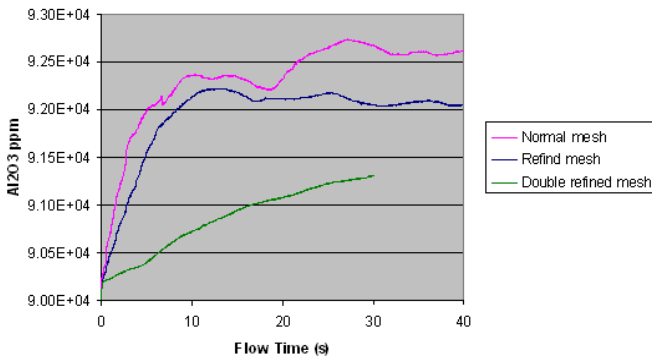


**Figure 8:** Mean Al<sub>2</sub>O<sub>3</sub> content in slag – time step for CEQCSI call: 0.05 s.

The main idea to determine the adequate Ceqcsi time step call consists in adjusting it with the species renewal time of the cell. If we keep in mind that the species renewal in a cell is limited by the vertical diffusion, then we should have:

$$(\Delta z)^2/\Delta t=D \text{ and } \Delta t \text{ is the renewal time.}$$

$\Delta t$  can be identified to the Ceqcsi time step call. Table 2 gives the  $\Delta t$  values when diffusion length is imposed to be the cell thickness.

**Table 2:** Adaptation of time step to call the thermodynamics model.

Cell thickness (mm)	4	2	1
Diffusivity (m <sup>2</sup> /s)	4 10 <sup>-5</sup>	2 10 <sup>-5</sup>	10 <sup>-5</sup>
Time step for Ceqcsi call (s)	0.4	0.2	0.1
Diffusion length (D $\Delta t$ ) <sup>0.5</sup> (mm)	4	2	1

Figure 9 shows that the superimposition of the curves is much better than previously. But, if we consider a realistic species diffusivity  $D \sim 3.0 \cdot 10^{-9} \text{ m}^2/\text{s}$ , the Ceqcsi time step should be 1h30 when  $\Delta z$  is 4 mm: it is not possible to have calculations for such long time and the numerical diffusions should overcome the molecular one. If cell thickness is 100  $\mu\text{m}$ , then  $\Delta t$  is 3 s, which is a realistic value on the CFD point of view, with the insurmountable drawback of huge number of cells for an industrial application.

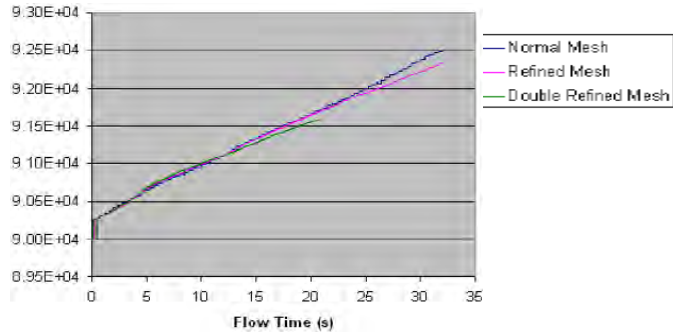


**Figure 9:** Mean Al<sub>2</sub>O<sub>3</sub> content in slag - results independent of mesh size.

At this moment, these calculations are possible on a qualitative point of view, using much larger species diffusivity than real ones, with cell thickness larger than 1 mm. Some trends will be obtained but the time evolution will be much quicker than what it should be. Nevertheless, the information we get is sufficient to classify the mutual influence of steel grades and initial slag composition on the slag viscosity. On an engineering point of view, the coupling between CFD and thermodynamics can be fruitfully used.

To get more realistic values of the time evolution of slag composition, another method should be used, which will be explained now.

## CAN WE USE CORRELATIONS BASED ON FLOW AND FLUID PROPERTIES TO EXTRACT THE MASS TRANSFER COEFFICIENT?

As it was already investigated by Calmet (1998) or Banerjee (2004), CFD can provide some valuable correlations to get the mass transfer coefficient  $\beta$ . For instance, the following relation can be considered (valid for  $Sc < 100$ ):

$$\beta Sc^{0.5} / u^* \sim 0.108 - 0.158$$

$$u^* = \sqrt{\frac{\tau_i}{\rho}} \quad \text{is the friction velocity} \quad (1)$$

where  $\tau_i = \mu \left( \frac{\partial u}{\partial n} \right)_i$  is the interface shear stress

or this one which was proposed by Banerjee, known as “surface-divergence” correlation:

$$\beta \approx Sc^{-1/2} u^* Re_t^{-1/2} \left[ \left( \frac{\partial u}{\partial x} + \frac{\partial v}{\partial y} \right)_i \right]^{1/4} \quad (2)$$

where  $Re_t = \Lambda u_{max} / \nu$  (the integral length scale of turbulence  $\Lambda$  is assimilated here to the height of liquid steel phase H or slag when slag is considered) and (x, y) plane is the interface plane.

When  $\beta$  and the interfacial area are known, Ceqcsi can calculate the time evolution of the slag composition. Interfacial area can be determined by VOF-PLIC method, see Figure 10, as soon as interface deformation is not too complex.

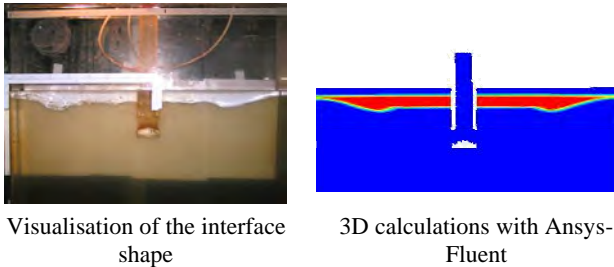


Figure 10: Schematic diagram of geometry.

But equation (1) or (2) cannot be used directly in our case since species  $Sc$  is around 1000 (value depending on species) and out of the validity range. A specific study should be carried out to extend the correlation up to  $Sc \sim 1000-2000$ . The method consists in performing two kinds of calculations:

1- a scalar value is imposed at the interface and scalar profile is drawn at different positions and times; the profile is then used to identify the mass transfer coefficient, as it was explained by Haroun (2008).

2- based on a sufficient number of previous calculations, scaling laws are built: for instance  $\beta_L \sim Sc^{-n}$  or  $\beta_L \sim u^{*m}$  ( $n = -1/2$  and  $m = 1$  for equation (1)).

Preliminary calculations were realised with Ansys-Fluent™ but, unfortunately, we did not manage to respect the interfacial shear stress continuity across a flat interface, even for very thin cells around 10  $\mu m$

thickness. It was the reason why we decided to switch to another CFD code: Thetis.

Thetis is developed at Institut de Mécanique et d'Ingénierie de Bordeaux, Trèfle department. It is devoted to the prediction of multiphase flow in laminar or turbulent situation and special emphasis is given to accurate description of interface tracking based on VOF method, see Vincent (2010).

A first set of calculations was realised in the case of a channel flow with two counter-current stratified fluids: liquid in the bottom and gas at the top. The momentum source is a pressure gradient in both fluids. Intensive CFD work was already realised by Fulgosi (2003) and Adjoua (2010): their work is considered as reference to test Thetis reliability. In Thetis, mesh refinement in the interface region is adapted to get at minimum 3 cells in the viscous sub-region. Dynamic LES turbulence model is used, without adaptation of the subgrid scale model at the interface. A very good agreement with results published by Adjoua was obtained (Figure 11) and interface shear stress continuity was respected.

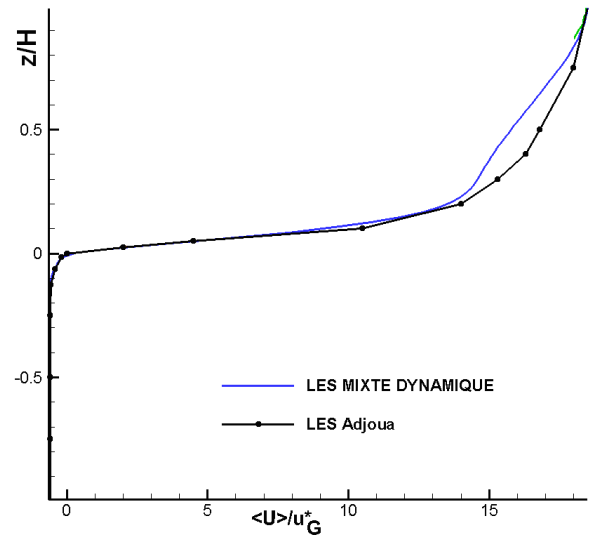


Figure 11: Dimensionless vertical coordinate according to mean velocity - comparison between LES model of Thetis and LES of Adjoua.

Since the good behaviour of Thetis was established, a second configuration was studied. It is still a channel flow but with liquid steel at the bottom and slag at the top.

The momentum source is a pressure gradient in the liquid steel phase and slag is entrained by the shear stress exerted at the interface (as it is in a real mould). The fluid properties are given in Table 3.

Table 3: Fluid properties.

	Steel	Slag
Density – kg/m <sup>3</sup>	7000	2500
Viscosity – Pa.s	0.00539	0.0539
Interface tension	1.2 N/m	

The boundary conditions are periodic in the streamwise and spanwise directions whereas symmetry conditions are imposed in the direction normal to the interface. The initial velocity guess is chosen as a fluctuating instantaneous field coming from the simulations of Adjoua after the turbulence was developed. The maximum liquid steel velocity is selected to be 0.3 m/s (close to what is measured in real continuous casting mould near the interface) and the height of the channel filled with liquid steel is 0.009576 m. Reynolds number is then 3730.

The mesh in the interface region is depending on Schmidt number, according to  $\delta_s \approx \delta_m Sc^{-1/3}$ . If  $Sc=1000$ , species boundary layer is 10 times lower than momentum one and much more cells are necessary to describe the species behaviour.

It is important to control that we have shear stress continuity across interface (see Table 4, transient calculations), which makes possible the calculation of the friction velocity on both sides of the interface.

**Table 4:** Shear stress and friction velocity at interface at different times.

	$\tau_{i,ls}$ (Pa)	$\tau_{i,sl}$ (Pa)	$u_{ls}^*$ (m/s)	$u_{sl}^*$ (m/s)
t=1.4s	0.46	0.48	0.0081	0.014
t=4s	0.23	0.26	0.0057	0.01
t=6s	0.22	0.22	0.0055	0.0092

Figure 11 displays the concentration field at time t=4 s, when the concentration at the interface is imposed to be 1, and makes explicit the need to refine the mesh depending on Schmidt number.

The interface is totally flat and aligned with the cells, which is very important to have negligible numerical diffusion. We checked that, in the case of laminar flow with very large  $Sc (>10^7)$ , the species diffusion in the vertical direction is totally negligible.

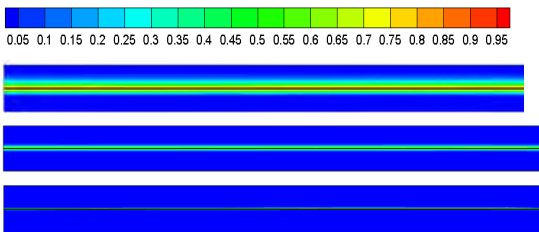


**Figure 11:** Mean species concentration at t=4 s, for Sc=10 (top), 100 (middle), 1000 (bottom).

Vertical concentration profiles are extracted, Figure 12.  $Z=0$  corresponds to interface position,  $z < 0$  is steel and  $z > 0$  is slag. Due to the fluid properties, diffusion is not symmetrical, with deeper diffusion when species diffusivity is higher, as it is the case for slag compared to steel.

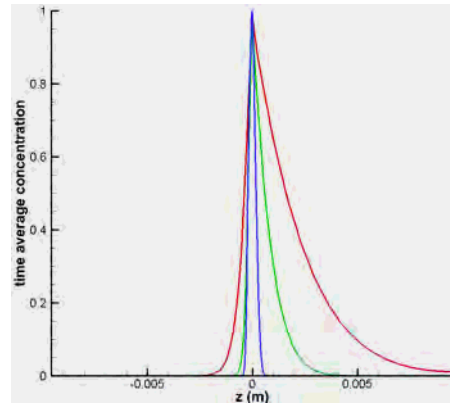


**Figure 12:** Vertical concentration profile at t=4 s, for Sc=10 (red), Sc=100 (green), Sc=1000 (blue).

The curves can be used to get the mass transfer coefficient, according to equation (3):

$$\beta = \frac{D \left( \frac{\partial C}{\partial z} \right)_i}{(C_i - C_\infty)} \quad (3)$$

Table 5 summarises the results. Higher mass transfer coefficient is confirmed at the slag side. Those values are referenced as “Steel-simulation” on Figure 13.

**Table 5:** Mass transfer coefficients, t=4 s.

	Mass transfer coefficient, steel side (m.s <sup>-1</sup> )	Mass transfer coefficient, slag side, (m.s <sup>-1</sup> )
Sc=10	4.94E-05	4.23E-04
Sc=100	1.16E-05	1.33E-04
Sc=1000	1.37E-06	2.81E-05

Then, mass transfers obtained with species diffusion were compared to the ones obtained using correlation, for instance equation (2) proposed by Banerjee.

Mass transfer coefficients obtained with (2) are referenced as “Steel-SD” in Figure 13.

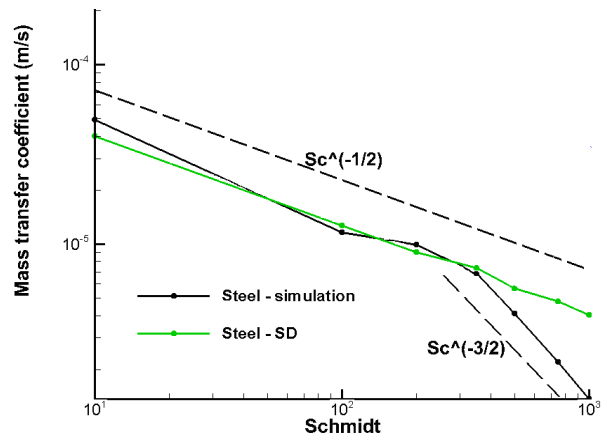


**Figure 13:** Dependence of mass transfer on Schmidt number, liquid steel side.

The main conclusions when we compare the two methods are:

▪up to  $Sc$  200-300, the two methods give similar results; it is very encouraging to note that the species diffusion method also provides the  $Sc^{-1/2}$  scaling law.

▪for large  $Sc$  ( $> 400$ ), which is our situation for steelmaking systems, we deviate from  $Sc^{-1/2}$  scaling law and have  $Sc^{-3/2}$ ; this new result needs to be investigated in more details to understand why the scaling law is depending on  $Sc$  with a rupture around  $Sc=350$ ; there are significant effects on a practical point of view, since low mass transfer coefficient is very detrimental for our process productivity.

▪standard correlations cannot be used but should be adapted for high  $Sc$  number; the species diffusion method proposed here is probably the good method to enlarge the validity range of the correlations, since the numerical diffusion is negligible; but we have to keep in mind that LES results should be compared to DNS to better assess the LES reliability near interface when typical length scales for species diffusion are much smaller than the viscous sublayer.

Further calculations were realised, with different interface frictions and Schmidt numbers. Then, a fitting function was built for both liquid steel and slag. Comparison is drawn on Figure 14 ( $u_{ls}^* = 0.0057$  m/s,  $u_{sl}^* = 0.0103$  m/s).

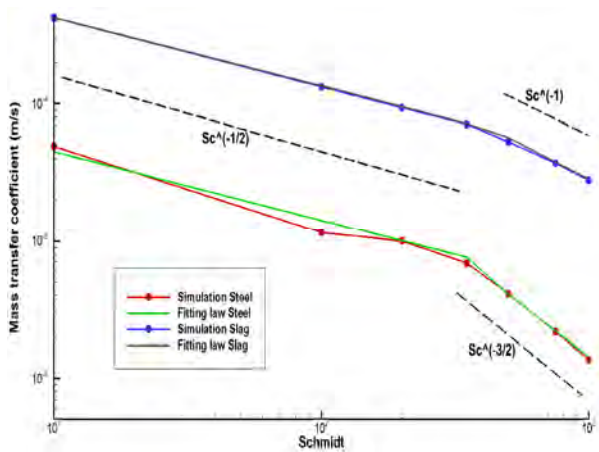


**Figure 14:** Dependence of mass transfer on Schmidt number, liquid steel and slag sides.

Below are the expressions of the fitting functions:

$$\beta_{ls} = u_{ls}^* (B_{ls} Sc^{-1/2} + E_{ls} Sc^{-3/2})$$

$$\beta_{sl} = u_{sl}^* (B_{sl} Sc^{-1/2} + E_{sl} Sc^{-1})$$

With :

$$B_{ls} = 0.025 I_{0-350}$$

$$E_{ls} = 8 I_{350-1000}$$

$$B_{sl} = 0.13 I_{0-350}$$

$$E_{sl} = 5 I_{350-1000}$$

$I_{0-350}$ ,  $I_{350-1000}$  are the characteristic Heavyside functions being equal to 1 on the interval and 0 elsewhere.

In the near future, we will have to consolidate those correlations and understand why they are slightly different in liquid steel and slag.

When the correlations are applied in the case of continuous casting mould, the shear stress between liquid steel and slag can be approximated using the assumption of flat free surface with no-slip boundary condition. Then the shear stress is in the range 1-10 Pa and mass transfer in the liquid steel side is approximately  $10^{-5}$  m/s (much smaller than in the slag side), which is coherent with values taken by Chaubal (1992).

## CONCLUSIONS

Coupling between fluid dynamics and thermodynamics was realised to predict chemical composition of both liquid steel and slag. To get rid of mesh size dependence, it was proposed to align the time step call to thermodynamic software with the typical diffusion time across the cell near the interface. This coupling can provide qualitative information on chemical evolution but is not suitable for quantitative prediction.

Improvement of the modelling is based on the prediction of the mass transfer coefficient  $\beta$ . Scalar diffusion method was used to calculate  $\beta$  for different Schmidt numbers. Classical dependence  $\beta / u^* \sim Sc^{-1/2}$  was predicted, but the scaling law was changed when  $Sc > 350$ . A correlation was proposed for both liquid steel and slag, to be applied in the range  $10 < Sc < 1000$ . Further work will be necessary to test the correlations but the order of magnitude is compatible with values already published.

## REFERENCES

- ADJOUA, S., (2010), "Développement d'une méthode de simulation de films cisailés par un courant gazeux", *Thesis report, Toulouse University*.
- ANDERSSON, M., HALLBERG, M., JONSSON, L., JÖNSSON, P., (2002), "Slag-metal reactions during ladle treatment with focus on desulphurisation", *Ironmaking & Steelmaking*, **29(3)**, 224-232.
- BANERJEE, S., LAKEHAL, D., M. FULGOSI, M., (2004), "Surface divergence models for scalar exchange between turbulent streams", *International Journal of Multiphase Flow*, **30**, 963-977.
- CALMET, I., MAGNAUDET, J., (1998), "High-Schmidt number mass transfer through turbulent gas-liquid interfaces", *International Journal of Heat and Fluid Flow*, **19**, 522-532.
- CHAUBAL, P., BOMMARAJU, R., (1992), "Development and use of a model to predict in-mould slag composition during the continuous casting of steel", *Steelmaking Conference Proceedings*, 665-675.
- DOOSTMOHAMMADI, H., ANDERSSON, M., KARASEV, A., JÖNSSON, P.G., (2010), "Use of Computational Thermodynamic Calculations in Studying the Slag/Steel Equilibrium during Vacuum Degassing", *steel research international*, **81(1)**, 31-39.
- FIGUEROA-ESPINOZA, B., LEGENDRE, D., (2010), "Mass or heat transfer from spheroidal gas bubbles rising through a stationary liquid", *Chemical Engineering Science*, **65**, 6296-6309.

FULGOSI, M., LAKEHAL, D., BANERJEE, S., DE ANGELIS, V., (2003), "Direct numerical simulation of turbulence in a sheared air-water flow with a deformable interface", *J. Fluid. Mech.*, **282**, 319-345.

GARDIN, P., SIMONNET, M., GAUTHIER, S., (2011), "Inclusion elimination in steelmaking ladle", *8th International Conference on CFD in Oil & Gas, Metallurgical and Process Industries, Trondheim*.

HAGEMANN, R., SCHWARZE, R., HELLERAND, H.P., SCHELLER, P.R., (2013), "Model Investigations on the Stability of the Steel-Slag Interface in Continuous-Casting Process", *Metallurgical and Materials Transactions B*, **44B**, 80-90.

HAROUN, Y., (2008), "Étude du transfert de masse réactif Gaz-Liquide le long de plans corrugués par simulation numérique avec suivi d'interface", *Thesis, University of Toulouse*.

JONSSON, L., SICHEN, D., JONSSON, P., (1998), "A New Approach to Model Sulphur Refining in a Gas-stirred Ladle- A Coupled CFD and Thermodynamic Model", *ISIJ International*, **38(3)**, 260-267.

LEHMANN, J., (2008), "Application of ArcelorMittal Maizières thermodynamic models to liquid steel elaboration", *Revue de Métallurgie*, **105 (11)**, 539-550.

PERICLEOUS, K., DJAMBAZOV, G., DOMGIN, J.F., GARDIN, P., (2008), "Dynamic modelling and validation of the metal/flux interface in continuous

casting", *6th European Conference on Continuous Casting 2008, Riccione*.

REAL-RAMIREZ, C.A., GONZALEZ-TREJO, J.I., (2011), "Analysis of three-dimensional vortices below the free surface in a continuous casting mold", *International Journal of Minerals, Metallurgy, and Materials*, 2011, **18(4)**, 397-407.

SHAHBAZIAN, F., SICHEN, D., SEETHARAMAN, S., (2002), "The effect of addition of Al<sub>2</sub>O<sub>3</sub> on the viscosity of CaO-FeO-SiO<sub>2</sub>-CaF<sub>2</sub> slags", *ISIJ International*, **42(2)**, 155-162.

VINCENT, S., BALMIGÈRE, G., CALTAGIRONE, J.P., MEILLOT, E., (2010), "Eulerian-Lagrangian multiscale methods for solving scalar equations - Application to incompressible two-phase flows", *J. Comput. Phys.*, **229**, 73-106.